INVITED PAPER *Special Section on Electronic Displays*

High Performance Organic Semiconductors with High Field-Effect Mobilities and Low Contact Resistances for Flexible Displays

Kota TERAI[†a)], **Emi KAWASHIMA**[†], **Naoki KURIHARA**[†], **Hideaki NAGASHIMA**[†], **Hirofumi KONDO**[†], **Masatoshi SAITO**[†], ***and*** **Hiroaki NAKAMURA**[†], ***Nonmembers***

SUMMARY We have succeeded in developing high-performance p-type of organic semiconductors with phenylethynyl groups, which have high filed-effect mobilities ($> 3\,cm^2V^{-1}s^{-1}$) by improving molecular planarity. A single crystal of the organic semiconductors has a herringbone structure. It plays an important role for carrier transport. In addition, we found that they had lower contact resistances to Au electrodes as well. Then, we used the materials for the carrier injection layer deposited onto another organic semiconductor we developed recently, which achieved a high field-effect mobility, and a low threshold voltage (V_{th}).

key words: *organic semiconductor, OTFT, herringbone structure, contact resistance*

1. Introduction

Organic thin film transistors (OTFTs) have several advantages for electronic devices, such as low cost, flexibility and light weight [1], [2]. Furthermore, it has attracted much attention in large-area applications including flexible circuits, such as sensors [3], light emitting diodes [4], solar cells [5], [6] and flexible displays [7] since it was found that field-effect mobilities of several compounds exceeded that of amorphous silicon.

We have been developing organic semiconductors for OTFTs and we reported oligo-*p*-phenylenevinylenes showed good performances. 1,4-Bis(4-methylstyryl) benzene (4MSB) has a high field-effect mobility of $0.13\,cm^2V^{-1}s^{-1}$ [8], [9]. However, an OTFT needs a higher field-effect mobility and a lower threshold voltage to be commercialized for flexible displays. In order to achieve a higher field-effect mobility, we focused on a molecular structure to improve the molecular design. As the result, we have succeeded in developing 2,6-Bis(2-phenylethynyl) anthracene (DPEA) as a new p-type of organic semiconductor which designed to improve planarity of a molecule.

In this report, we studied material properties, such as crystal structure of single crystals, growth mechanism of thin films and contact resistances (R_Cs) to achieve the high field-effect mobility of over $3\,cm^2V^{-1}S^{-1}$. In addition, DPEA was found to have good carrier injection characteristics by R_C measurement. We fabricated OTFT devices with the DPEA as a carrier injection layer on the other organic semiconductor.

Manuscript received March 24, 2011.
Manuscript revised June 7, 2011.

[†]The authors are with Idemitsu Kosan Co., Ltd., Sodegaurashi, 299-0293 Japan.
a) E-mail: kota.terai@si.idemitsu.co.jp

DOI: 10.1587/transele.E94.C.1713

2. Experiments

4MSB was purchased from Tokyo Chemical Industry Co., and DPEA was synthesized using Sonogashira coupling reaction. The chemical structures of 4MSB and DPEA are shown in Fig. 1. All of the semiconductors were purified by train sublimation under high vacuum of 7.0×10^{-6} Pa. The purity was evaluated to exceed 99% measured by high performance liquid chromatography (HPLC).

Single crystals of the organic semiconductors which were suitable for X-ray analysis were obtained by the following sublimation method: the materials were placed inside an edge of glass tubes (630 mm in length and 28 mm in diameter). The tubes were evacuated and the air was replaced with nitrogen. The tubes were sealed under pressure of around 0.1 atm and then the source materials were heated to 260°C for 4MSB and 240°C for DPEA respectively and 150°C at the other edge. X-ray diffraction (XRD) data on single crystals were measured by a Rigaku AFC10 diffractometer (Mo-Kα radiation, $\lambda = 0.71070$ Å, graphite monochromated). The single-crystal structures were solved by direct methods. Non-hydrogen atoms were refined anisotropically, and all hydrogen atoms were inserted at calculated positions. By using the result of the single crystal analysis, all calculations were performed using the crystallographic software package Crystal Structure Version 2.00. The bandwidths were calculated with framework of the tight-binding theory as proposed by Brédas and co-workers [10], using the semiempirical intermediate neglect of differential overlap (INDO) method employed in Gaussian 03 [11].

We fabricated top-contact OTFTs as shown in Fig. 2, using two types of substrates. One is a glass substrate with a poly (chloro-*p*-xylylene) (Parylene-C) insulator [12], the other one is a Si substrate with a thermal oxidized SiO_2 gate insulator (300 nm). In the case of Si substrate, a SiO_2 surface was treated by hexamethyldisilazane (HMDS) [13] or polystyrene (PS) [14] with a thickness of 20 nm to obtain

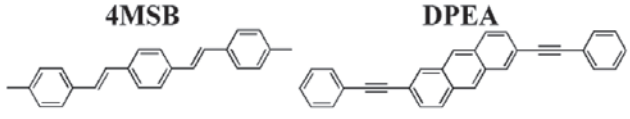

Fig. 1 Chemical structure of 4MSB and DPEA.

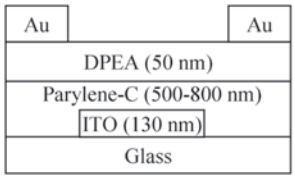

Fig. 2 Illustration of the top-contact device structure on the glass substrates.

a lower surface energy. The organic semiconductors were evaporated under a pressure of below 2×10^{-4} Pa at a deposition rate of 0.05 nm/s to form a layer with a thickness of 40–50 nm on the substrate at room temperature. Au source-drain electrodes were evaporated through a shadow mask with a thickness of 50 nm on the semiconductor. The channel length L and width W were 50 μm and 1 mm, respectively. In the case of a glass substrate, we used an indium-tin-oxide (ITO) layer sputtered onto a glass substrate with a thickness of 130 nm as a gate electrode. The ITO film was patterned by a conventional photolithography technique to form 6-mm-wide, 25-mm-length stripes. Subsequently, the Parylene-C was deposited by thermal chemical vapor deposition at a thickness ranging from 500 to 800 nm to serve as a gate insulator. The organic semiconductors and the electrodes fabricated under the same conditions as that in the case of the Si substrate. The fabricated devices annealed at 100°C in 3 hours in a glove box with under N_2 atmosphere.

All devices were temporarily exposed to air prior to conducting measurement and the measurement was conducted under vacuum conditions using Keithley 4200SCS Semiconductor Parameter Analyzer.

The electric parameters were estimated in OTFTs using a standard analytic theory of metal-oxide-semiconductor field-effect transistor. Above threshold voltage, the drain current tends to saturate due to the pinch off of accumulation layer, and is modeled by

$$I_D = \frac{WC}{2L}\mu(V_G - V_T)^2, \tag{1}$$

where, W and L are the channel width and length, C is the capacitance per unit area of the insulator, V_G and V_T are the gate and threshold voltage and μ is the field-effect mobility in channel regime. The field-effect mobility can be calculated from the slope of the plot of $|I_D|^{1/2}$ versus V_G.

The contact resistances between the electrode/semiconductor interfaces were evaluated by the transmission line model (TLM) [15]–[17]. We fabricated six devices having an identical channel width (2 mm) and varied channel length (L = 50–300 μm). DPEA and pentacene were deposited as semiconductor onto Prylene-C insulator. Figure 3 shows an optical micrograph of a device for TLM measurement with different channel length and a schematic illustration of transistor with cross section describing R_C.

In the linear regime, the total resistance (R_{tot}) of an OTFT can be explained as the sum of channel resistance (R_{ch}) and R_C as below

$$R_{tot} = R_c + R_{ch}, \tag{2}$$

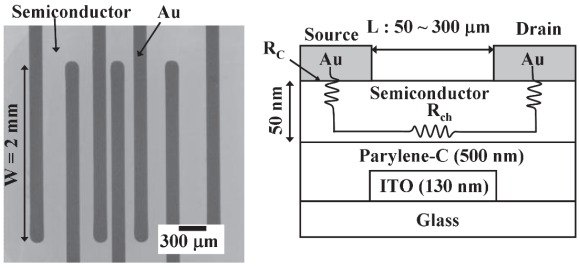

Fig. 3 Optical micrograph of TLM device (left) and schematic transistor cross section describing R_C (right).

$$R_{ch} = \frac{L}{\mu WC(V_G - V_T)}. \tag{3}$$

This equation indicates that we can obtain R_C by extrapolation of L to zero along the line of the channel length dependence of R_{tot}.

Crystal structures in thin films on OTFTs was measured by a Rigaku RINT-III diffractometer (Cu-Kα radiation, λ = 1.54184 Å, graphite monochromated).

An ionization energy (Ip) of vacuum-evaporated films on ITO electrodes was measured using AC-3 photoelectron yield spectroscopy in air (Riken Keiki).

Surface morphologies observation is measured by using an atomic force microscope (AFM) from SII NanoTechnology Inc. (SPA400).

3. Results and Discussions

3.1 Single Crystal Structure and Theoretical Calculation

First, we determined single crystal structures of 4MSB and DPEA by X-ray scattering. As shown in Fig. 4, 4MSB has a steric hindrance between the hydrogen atoms of the phenyl groups and the hydrogen atoms of the double bonds. Therefore, the molecule of 4MSB is slightly twisted from the planar structure. On the other hand in DPEA, an anthracene group and a phenyl group are linked via a triple bond, and the both groups have enough distance to avoid steric hindrance.

Consequently, the molecule of DPEA has the planar structure, which is expected to have a higher mobility due to the improvement of the molecular packing by the strong interaction between molecules.

Figure 5 and Fig. 6 show the crystal packing projected along the c-axis and the b-axis, respectively. All single crystals have herringbone structures and a layered structure similar to the crystal structure of pentacene.

Then, we performed semiempirical INDO calculations for the molecular geometries extracted from single-crystal analysis. Table 1 shows Highest Occupied Molecular Orbital (HOMO) bandwidths of 4MSB and DPEA along a herringbone arrangement (arrow A) and along a b-axis (arrow B), which are calculated to be 264, 315 and 53, 252 meV, respectively. In general, materials which have wide bandwidths indicate a high electronic conductivity. DPEA shows

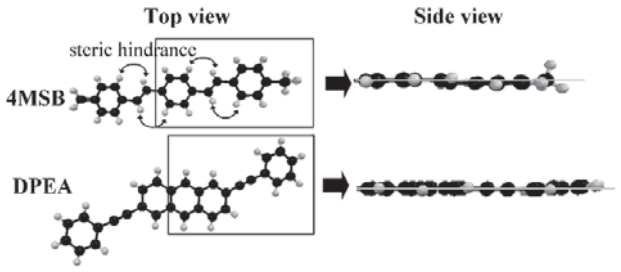

Fig. 4 Top and side view of molecules of 4MSB and DPEA.

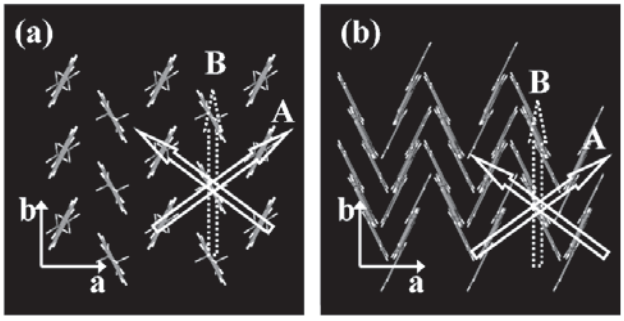

Fig. 5 Crystal structure of (a) 4MSB and (b) DPEA projected along the *c*-axis. Arrow A corresponds to herringbone arrangement, and arrow B corresponds to the *b*-axis.

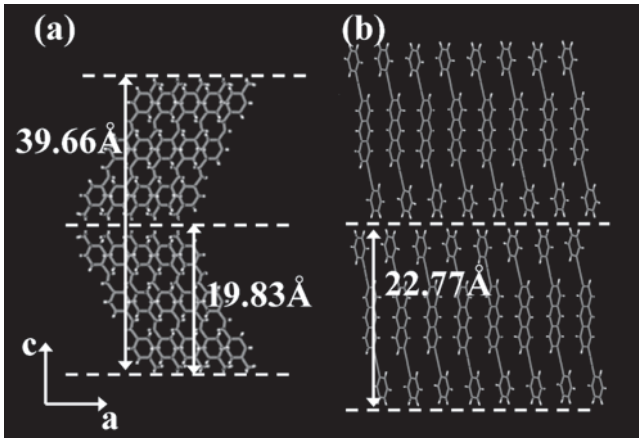

Fig. 6 Crystal structure of (a) 4MSB and (b) DPEA projected along the *b*-axis.

Table 1 Bandwidth of HOMO level by INDO.

	4MSB	DPEA	Pentacene
Nearest neighbor A (meV)	264	315	320
Nearest neighbor B (meV)	53	252	158

similar band width with pentacene as shown in Table 1. DPEA is expected to have a high field-effect mobility similar to pentacene.

In our study, the semiconductor layers in the OTFTs were polycrystalline films. We measured crystallinity by

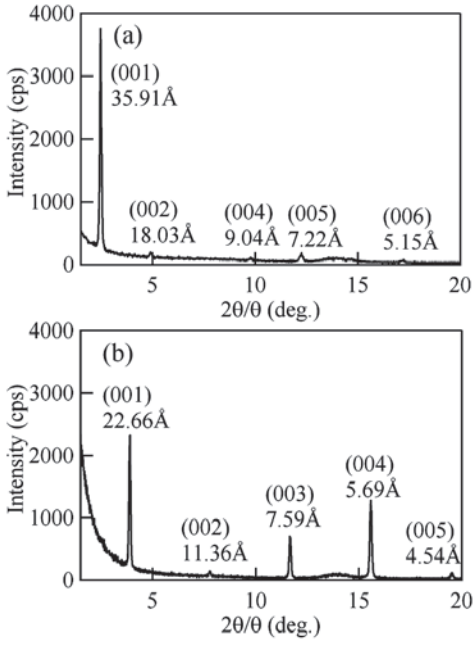

Fig. 7 XRD patterns of (a) 4MSB and (b) DPEA films vacuum-evaporated onto Parylene-C coated glass substrates.

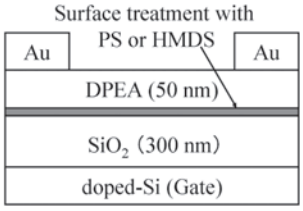

Fig. 8 Illustration of the top-contact device structure on the Si substrates.

Table 2 OTFTs properties with DPEA semiconductor layer on different surface. ($V_D = -100$ V)

	SiO_2/PS	SiO_2/HMDS	Parylene-C (800 nm)
μ ($cm^2V^{-1}s^{-1}$)	3.5	0.09	0.89
V_{th} (V)	-41	-9.3	-42
$I_{on/off}$	8.2 X 10^6	4.1 X 10^4	3.2 X 10^6

XRD to confirm that the thin film have the same structure with the single crystal structures. Figure 7 shows XRD spectra of organic semiconductors on the Parylene-C insulator. The 4MSB and DPEA thin films indicate strong scattering with highly *c*-axis oriented structure. In addition, both of a lattice constant of thin films (*c*-axis) are similar to the results of the calculation from the single crystals. Therefore, the grains in the films are assumed to be single crystal like.

3.2 Device Performance

Next, device performances are discussed. Figure 8 shows a device structure of an OTFT on a Si substrate. Table 2 shows OTFT characteristics for each device. Compared

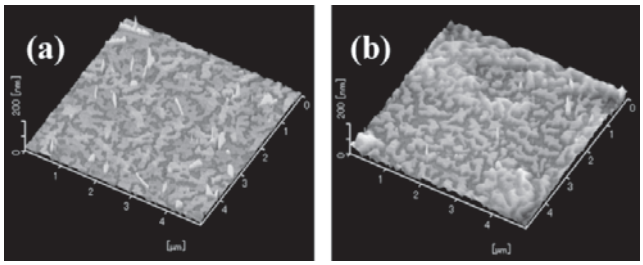

Fig. 9 AFM images of DPEA (10 nm) thin films on (a) PS treated and (b) HMDS treated surface.

with the HMDS treatment, the OTFT with the PS treatment showed the good performance with a field-effect mobility of $3.5\,\mathrm{cm^2V^{-1}s^{-1}}$ at $V_D = -100\,\mathrm{V}$ and an on/off ratio of 8.2×10^6.

In general, carrier mobilities of organic materials depend on their crystal structures and grain morphologies [18]. We measured surface morphologies of the films with a thickness of 10 nm to confirm an effect of the surface treatment of SiO_2. Figure 9 shows the surface morphologies of the DPEA films on SiO_2 gate insulator treated with PS and HMDS which measured by AFM. The DPEA film on the substrate treated with PS showed larger coverage than that on the substrate treated with HMDS. These results suggest that the high field-effect mobility in DPEA devices is caused by the continuity of the thin films at the channel region besides the crystal structure as above mentioned.

As shown in Table 2, DPEA shows high potential as a semiconductor. However, this high mobility was obtained under a large drain-voltage (V_D), and the V_T was also high to be commercialized for flexible displays. One method to decrease the driving voltage is to improve the capacity of the insulator film. Therefore, the thickness of the Parylene-*C* was reduced form 800 nm to 500 nm to increase a capacitance.

Figure 10 shows device characteristic of the device with DPEA on Parylene-C insulator. The field-effect mobility and the threshold voltage were calculated to be $0.25\,\mathrm{cm^2V^{-1}s^{-1}}$ and −9.5 V, respectively. In low drain voltage region of transfer characteristics (Fig. 10(b)), the turn on voltage is found to be close zero. This result suggests that the R_C of DPEA is small.

In order to clarify the relationship between the carrier injection and R_C, we evaluated R_C by TLM method [15]–[17]. Figure 11 shows that the R_C of the DPEA device is smaller than that of the pentacene device, which is responsible to the good carrier injection. The R_Cs of DPEA and pentacene are 4 and 92 kΩcm respectively. To our knowledge, this value of the R_C of DPEA is one of the smallest value of R_Cs at the interface with Au. In the case of pentacene, it shows a large R_C. In past reports, pentacene shows a large R_C in the same range of our works [15]–[17].

Comparison R_C between DPEA and pentacene is discussed. The Ip of DPEA and pentacene lies at 5.4 and 5.1 eV respectively and the work function (WF) of Au lies at 5.1 eV. Therefore, pentacene has an advantage for the hole injection

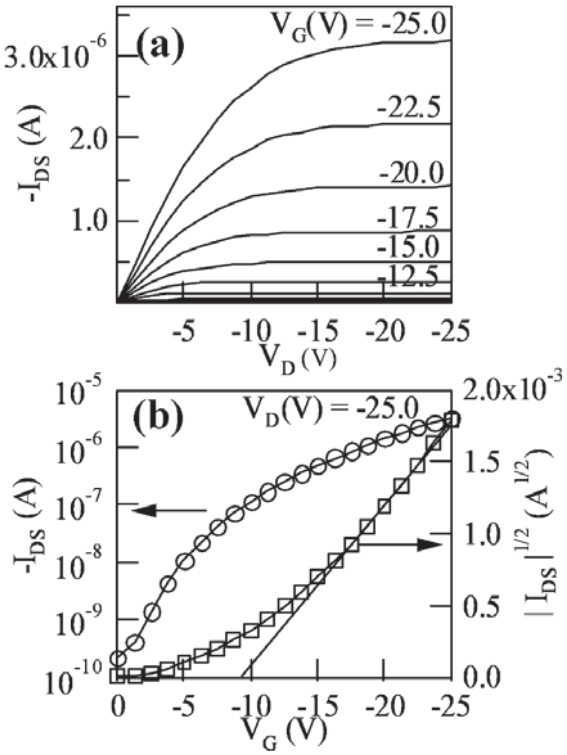

Fig. 10 (a) Plots of the I_D vs V_D at carious V_G calues for the OTFT using DPEA as a semiconductor. (b) Transfer characteristics of OTFT with DPEA on Parylene-C insulator. ($V_D = -25\,\mathrm{V}$)

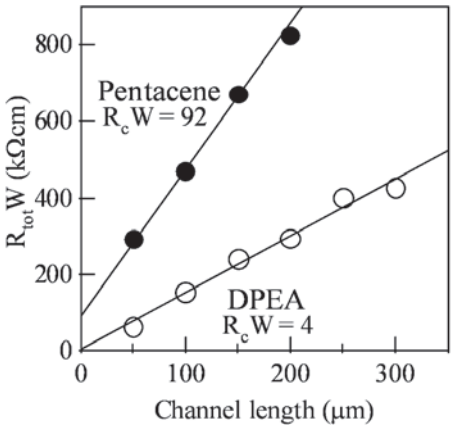

Fig. 11 Channel width normalized total resistance ($R_{tot}W$) versus channel length of Au/Pentacene and Au/DPEA devices. (TLM plots calculated at $V_D = -5\,\mathrm{V}$ and $V_G = -80\,\mathrm{V}$)

from the view point at the energy level. However, the R_C of pentacene is larger than that of DPEA in our result. In general, characteristics of a organic semiconductor could be changes by exposing to air. One effect is to dope holes by absorbing oxygen molecules [19]–[21].

On the other hand, the large R_C of pentacene might be caused by a hole trap state [22]. Wang et al. discussing about a contact resistance instability in pentacene OTFTs [19], [23]. These reports suggest that an H_2O adsorption leads to the R_C increase because of a generation of hole trap states.

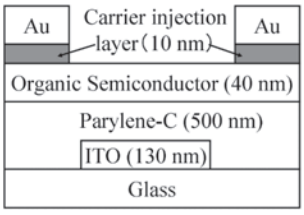

Fig. 12 OTFTs device structure with carrier injection layer.

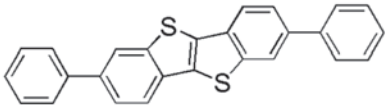

Fig. 13 Chemical structure of DPh-BTBT.

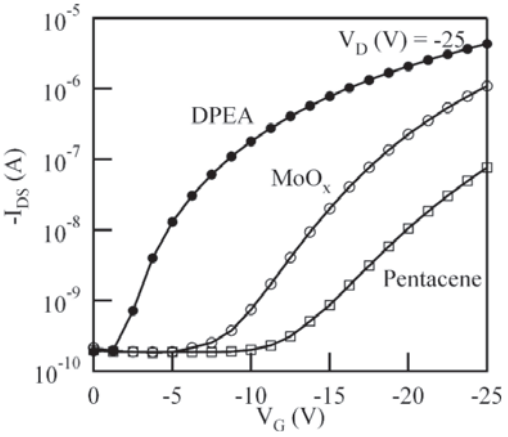

Fig. 14 Transfer characteristics of OTFTs with different carrier injection layers on DPh-BTBT. ($V_D = -25$ V)

We guess that the increasing of resistance at the pentacene caused by the hole traps. The difference between DPEA and pentacene of R_C may be due to the difference of Ip.

This result suggests that DPEA is effective material in the carrier injection.

3.3 DPEA Carrier Injection Layer

Finally, focusing on the low R_C at the interface between DPEA and Au, we tried to fabricate high performance OTFTs with a top contact structure using DEPA as a carrier injection layer. A device structure with a carrier injection layer is shown in Fig. 12. The thicknesses of injection layer and Au films were 10 and 50 nm, respectively. We used 2,7-diphenyl[1]benzothieno[3,3-b]-[1]benzothiophene (DPh-BTBT) which was reported as the material with a high Ip (5.6 eV) and a high mobility [24]. A chemical structure of DPh-BTBT is illustrated in Fig. 13. MoO_x [23], [25] and pentacene were used as the carrier injection materials to compare with DPEA.

Figure 14 shows transfer characteristics of the DPh-BTBT devices with MoO_x, pentacene and DPEA as the carrier injection layer, respectively. The electrical characteristics of the OTFTs with different carrier injection layers in this study are summarized in Table 3. The transfer characteristics clearly show that the turn-on voltage decreased to around 0 V in the OTFTs with the DPEA layer. The device with the DPEA layer showed the highest performance with a field-effect mobility of 0.30 $cm^2V^{-1}s^{-1}$ and the V_{th} is −8.3 V. These results demonstrate that DPEA played an important role to reduce the driving voltage.

Table 3 Electrical characteristics of the OTFTs with carious carrier injection layers. ($V_D = -25$ V)

semiconductor	DPh-BTBT		
Injection layer	DPEA	pentacene	MoO_x
μ ($cm^2V^{-1}s^{-1}$)	0.3	0.03	0.08
V_{th} (V)	-8.3	-13.9	-13.6

In the case of MoO_x as the carrier injection layer, the enhancement of carrier injection by MoO_x in OTFT and OLED have reported in many groups [23], [25]–[27]. The mechanism of carrier injection is explained by a carrier generation at the interface. It is assumed that the enhancement of drain current of the device with MO_x as attributed to the same effect.

Comparison between DPEA and pentacene as a carrier injection layer is discussed. In order to understand the effect of DPEA as a carrier injection layer, we considered alignment of energy levels for DPh-BTBT [28], [29], pentacene, DPEA, and Au. Figure 15 shows an illustration of energy diagrams to explain the carrier injection through injection layers into the DPh-BTBT layer. The Ip of pentacene lies at 5.1 eV and is close with the WF of Au, resulting in a large barrier for injection into the DPh-BTBT layer (see Fig. 15(a)). On the other hand, the Ip of DPEA lies at 5.4 eV which is located between the WF of Au and the Ip of DPh-BTBT (see Fig. 15(b)). Therefore, the carrier injection of the DPEA to the DPh-BTBT is more effective than that of the pentacene from the alignment of the energy level. Moreover, the R_C of DPEA is smaller than that of pentacene and is improving a drain current of OTFT as mentioned above. DPEA has a large advantage.

In our studies, the mechanism of carrier injection is not fully explained. We need further study about the carrier generation in DPEA to understand the enhanced carrier injection.

Then, we tried to fabricate an OTFT with higher performance OTFTs using other organic semiconductors. The characteristics of the OTFT with DPEA as a carrier injection layer shows uniformly improved threshold voltage. In the case of a newly synthesized semiconductor, we have succeeded in obtaining a high field-effect mobility (> 7 $cm^2V^{-1}s^{-1}$) and now in developing.

4. Conclusion

A new type of organic semiconductor has been introduced. DPEA is expected to have higher mobility form the crystallographic analysis and the calculation of bandwidth. Actu-

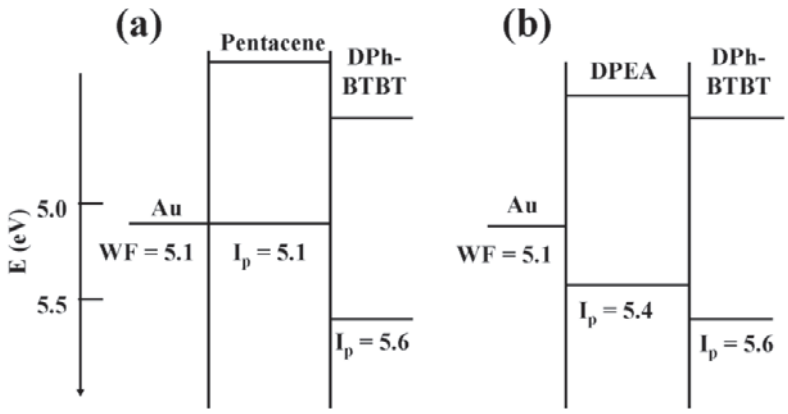

Fig. 15 Energy diagrams in interface of (a) pentacen/DPh-BTBT, (b) DPEA/DPh-BTBT.

ally the OTFT on PS treatment surface showed the high performance with a field-effect mobility of $3.5\,cm^2V^{-1}s^{-1}$ and an on/off ratio of 8.2×10^6. AFM results suggest that the high field-effect mobility in DPEA devices is obtained by the continuity of the thin film. These DPEA films showed low R_C by the TLM measurement. We have succeeded in fabricating OTFTs which have the high field-effect mobility and the low contact resistance by using DPEA as the carrier injection layer. We conclude that this work is a big step to achieve a high-performance flexible display.

References

[1] G. Horrowitz, "Organic field-effect transistors," Adv. Mater., vol.10, no.5, pp.365–377, 1998.
[2] C.D. Dimitrakopoulos and P.R.L. Malenfant, "Organic thin film transistors for large area electronics," Adv. Mater., vol.14, no.2, pp.99–117, 2002.
[3] S.C.B. Mannsfeld, B.C.-K. Tee, R.M. Stoltenberg, C.V.H-H. Chen, S. Barman, B.V.O. Muir, A.N. Sokolov, C. Reese, and Z. Bao, "Highly sensitive flexible pressure sensors with microstructured rubber dielectric layers," Nature Mater., vol.9 pp.856–864, 2010.
[4] J.H. Burroughes, D.D.C. Bradley, A.R. Brown, R.N. Marks, K. Mackay, R.H. Friend, P.L. Burns, and A.B. Holmes, "Light-emitting diodes based on conjugated polymers," Nature, vol.347, pp.539–541, 1990.
[5] P. Peumans, A. Yakimov, and S.R. Forrest, "Small molecular weight organic thin-film photodetectors and solar cells," J. Appl. Phys., vol.93, no.7, 3693, 2003.
[6] S. Günes, H. Neugebauer, and N.S. Sariciftci, "Conjugated polymer-based organic solar cells," Chem. Rev., vol.107, pp.1324–1338, 2007.
[7] G.H. Gelinck, H.E.A. Huitema, E. van Veenendaal, E. Cantatore, L. Schrijnemakers, J.B.P.H. van der Putten, T.C.T. Geuns, M. Beenhakkers, J.B. Giesbers, B.-H. Huisman, E.J. Meijer, E.M. Benito, F.J. Touwslager, A.W. Marsman, B.J.E. van Rens, and D.M. de Leeuw, "Flexible active-matrix displays and shift registers based on solution-processed organic transistors," Nature Mater., vol.3, pp.106–110, 2004.
[8] T. Yasuda, M. Saito, H. Nakamura, and T. Tsutsui, "Control of p- and n-type carriers by end-group substitution in oligo-*p*-phenylenevinylene-based organic field-effect transistors," Appl. Phys. Lett., vol.89, 182108, 2006.
[9] T. Yasuda, M. Saito, H. Nakamura, and T. Tsutsui, "Organic field-effect transistors based on oligo-*p*-phenylenevinylene derivatives," Jpn. J. Appl. Phys., vol.45, no.11, pp.L313–315, 2006.
[10] J. Cornil, J. Ph. Calbert, and J.L. Brédas, "Electronic structure of the pentacene single crystal: Relation to transport properties," J. Am. Chem. Soc., vol.123, 1250, 2001.
[11] H. Nagashima, M. Saito, H. Nakamura, T. Yasuda, and T. Tsutsui, "Organic field-effect transistors based on naphthyl end-capped divinylbenzene: Performance, stability and molecular packing," Org. Electron., vol.11, pp.658–663, 2010.
[12] T. Yasuda, K. Fujita, H. Nakashima, and T. Tsutsui, "Organic field-effect transistors with gate dielectric films of poly-*p*-xylylene derivatives prepared by chemical vapor deposition," Jpn. J. Appl. Phys., vol.42, pp.6614–6618, 2003.
[13] H. Yang, T.J. Shin, M.-M. Ling, K. Cho, C.Y. Ryu, and Z. Bao, "Conducting AFM and 2D GIXD studies on pentacene thin films," J. Am. Chem. Soc., vol.127, pp.11542–11543, 2005.
[14] G. Nunes, Jr., S.G. Zane, and J.S. Methb, "Styrenic polymers as gate dielectrics for pentacene field-effect transistors," J. Appl. Phys., vol.98, 104503, 2005.
[15] T. Minari, T. Miyadera, K. Tsukagoshi, and Y. Aoyagi, "Charge injection process in organic field-effect transistors," Appl. Phys. Lett., vol.91, 053508, 2007.
[16] S.D. Wang, T. Minari, T. Miyadera, Y. Aoyagi, and K. Tsukagoshi, "Bias stress instability in pentacene thin film transistors: Contact resistance change and channel threshold voltage shift," Appl. Phys. Lett., vol.92, 063305, 2008.
[17] S.D. Wang, T. Minari, T. Miyadera, K. Tsukagoshi, and Y. Aoyagi, "Contact-metal dependent current injection in pentacene thin-film transistor," Appl. Phys. Lett., vol.91, 203508, 2007.
[18] S.D. Wang, T. Miyadera, T. Minari, Y. Aoyagi, and K. Tsukagoshi, "Correlation between grain size and device parameters in pentacene thin film transistors," Appl. Phys. Lett., vol.93, 043311, 2008.
[19] S.D. Wang, T. Minari, T. Miyadera, K. Tsukagoshi, and J.X. Tang, "Contact resistance instability in pentacene thin films transistors induced by ambient gases," Appl. Phys. Lett., vol.94, 083309, 2009.
[20] F.D. Angelis, S. Cipolloni, L. Mariucci, and G. Fortunato, "Aging effects in pentacene thin-film transistors: Analysis of the density of states modification," Appl. Phys. Lett., vol.88, 193508, 2006.
[21] C. Vaterlein, B. Ziegler, W. Gebauer, H. Neureiter, M. Stoldt, M.S. Weaver, P. Bauerle, M. Sokolowski, D.D.C. Bradley, and E. Umbach, "Elecrtrical conductivity and oxygen doping of vapour-deposited oligothiophene films," Synth. Met., vol.76, pp.133–136, 1996.
[22] C. Goldmann, D.J. Dundlach, and B. Batlogg, "Evidence of water-related discrete trap state formation in pentacene single-crystal field-effect transistors," Appl. Phys. Lett., vol.88, 063501, 2006.
[23] M. Kano, T. Minari, and K. Tsukagoshi, "Improvement of subthreshold current transport by contact interface modification in p-type organic field-effect transistors," Appl. Phys. Lett., vol.94, 143304, 2009.

[24] K. Takimiya, H. Ebata, K. Sakamoto, T. Izawa, T. Otsubo, and Y. Kunugi, "2, 7-Diphenyl[1]benzothieno[3, 2-b]benzothiophene, A New Organic Semiconductor for Air-Stable Organic Field-Effect Transistors with Mobilities up to 2.0 $cm^2V^{-1}s^{-1}$," J. Am. Chem. Soc., vol.128, pp.12604–12605, 2006.
[25] C.-W. Chu, S.-H. Li, C.-W. Chen, V. Shrotriya, and Y. Yang, "High-performance organic thin-film transistors with metal oxide/metal bilayer electrode," Appl. Phys. Lett., vol.87, 193508, 2005.
[26] H. Nakanotani, M. Saito, H. Nakamura, and C. Adachi, "Tuning of threshold voltage by interfacial cattier doping in organic single crystal ambipolar light-emitting transistors and their bright electroluminescence," Appl. Phys. Lett., vol.95, 103307, 2009.
[27] T. Matsushima, G.-H. Jin, Y. Kanai, T. Yokota, S. Kitada, T. Kishi, and H. Murata, "Interfacial charge transfer and charge generation in organic electronic devices," Org. Electron., vol.12, pp.520–528, 2011.
[28] T. Ashimine, T. Yasuda, M. Saito, H. Nakamura, and T. Tsutsui, "Air stability of p-channel organic field-effect transistors based on Oligo-*p*-phenylenevinylene derivatives," Jpn. J. Appl. Phys., vol.47, no.3, pp.1760–1762, 2009.
[29] I. Osaka, T. Abe, S. Shinamura, E. Miyazaki, and K. Takimiya, "High–mobility semiconducting Naphthodithiophene copolymers," J. Am. Chem. Soc., vol.132, pp.5000–5001, 2010.

Kota Terai earned his Ph.D. on Material Engineering at Tokyo institute of technology in 2003. He has studied the application of oxide thin films. During 2003 to 2007, he joined Japan atomic energy agency in a post-doctoral researcher. He joined Idemitsu Kosan Co., Ltd. in 2007. Then he has been engaged in the research and development of organic semiconductors for a flexible display. Now he actively works for resolution of a number of issues such as carrier injection and instability of characteristics.

Emi Kawashima received the master degree in physics from Aoyama Gakuin University in 2009. She has studied the magnetic properties of intermetallic compounds. She joined Idemitsu Kosan Co., Ltd., in 2009. Now she is engaged in the research and development of organic and inorganic TFT materials.

Naoki Kurihara received the master degree in Physical Chemistry from Kyushu University, Japan, in 2008. He has studied the single-walled carbon nanotube field-effect transistors. He joined Idemitsu Kosan Co., Ltd., Japan, in 2008. Since then, he has been engaged in the research and development of organic TFT materials.

Hideaki Nagashima received his Ph.D. degree in Applied Chemistry in 2004 from Keio University working in the area of molecular magnetism. He had studied syntheses, physicochemical properties, crystal structure analyses, and quantum chemical calculations of organic free radicals. He joined Idemitsu Kosan Co., Ltd. in 2004. His current work is focused on device physics, photochemistry, and material design of phosphorescent OLED devices.

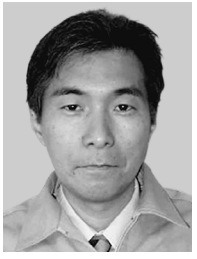

Hirofumi Kondo received his M.S. in Electrical Engineering at Tohoku University, Japan, in 1991. After graduation he joined Idemitsu Kosan Co., Ltd. His major research interests have been the printing process of organic materials (Liquid Crystal, OLED, OTFT) and characterization of those devices.

Masatoshi Saito joined Idemitsu Kosan Co., Ltd. In 1994 after graduating from School of Science, the University of Tokyo with a Ph.D. degree in Chemistry. After the research of functional materials, he has been engaged in the development of OTFTs materials since 2005. His major is molecular design and synthesis of organic materials.

Hiroaki Nakamura has been studying organic materials for electronics, such as OLED, OTFT and OPV since he joined Idemitsu Kosan Co., Ltd. in 1985 after graduating from Kyushu university with a master degree in physics. He received his Ph.D. at Kyushu university in 2008 on organic electronics for his research results. He is currently one of representative researchers in organic electronics field and now engaged in printed electronics.